

mega-telescopes and their IR instrumentation it will be possible to investigate the physical characteristics of these objects, particularly those in orbit around nearby stars which will allow us to obtain their masses. ALMA will be a perfect instrument for the follow-up studies of brown dwarfs found in these studies.

• *Extrasolar planets and proto-planetary disks.* – One of the great appeals of astronomy is undoubtedly its potential to help us understand the origin of our planet. The Centre will foster the development of the area of planetary science, currently non-existent in the country, starting from available human resources. This would be accomplished by joining and developing searches for extrasolar planetary systems using

modern techniques such as radial velocities, planetary occultations (transits) and micro-lensing. Once ALMA is available we will be able to undertake molecular line observations of the atmospheres of planets and other bodies which will give new knowledge of planetary “weather”, the structure of atmospheric wind and the variations in chemical constituents. Studies of proto-planetary disks will be carried out using the recently available IR facilities. ALMA, with its sensitivity and resolving power, will be the ideal instrument to provide definite answers regarding the formation and evolution of proto-planetary disks. Their images will have enough detail to allow astronomers to see chemical variations in proto-planetary systems and to permit them to compare

such systems with evolutionary models of our own solar system.

*The present article could not have been written without the contribution of the FONDAP Centre of Excellence Director, Guido Garay, and of its P.I. Members. I thankfully acknowledge the contribution from M.T. Ruiz, Director of the Astronomy Department at Universidad de Chile; L. Infante, Chairman of the Pontificia Universidad Católica de Chile Department of Astronomy and Astrophysics; W. Gieren, Head of the Astronomy Group at the Universidad de Concepción Physics Department; L. Barrera, from the Instituto de Astronomía at Universidad Católica de Antofagasta; and A. Ramírez, from Universidad de La Serena.*

## Dynamics and Mass of the Shapley Supercluster, the Largest Bound Structure in the Local Universe

A. REISENEGGER<sup>1</sup>, H. QUINTANA<sup>1</sup>, D. PROUST<sup>2</sup>, and E. SLEZAK<sup>3</sup>  
areisene@astro.puc.cl

<sup>1</sup>Departamento de Astronomía y Astrofísica, Facultad de Física, Pontificia Universidad Católica de Chile, Chile

<sup>2</sup>DAEC – Observatoire de Meudon, France

<sup>3</sup>Observatoire de la Côte d’Azur, France

### Introduction

The Shapley Supercluster is the largest bound structure identified in the local Universe ( $z < 0.1$ ). In this article, we discuss the role of superclusters as present-day “turning points” in the growth of structure in the Universe. We review observations of the Shapley Supercluster and their interpretation, particularly with regard to its dynamics and the determination of its mass, much of which has been done by our group, centred at Pontificia Universidad Católica de Chile. Finally, we describe our recent application of a spherical collapse model to the supercluster, and discuss possibilities of future progress.

### 1. Cosmological Structure Formation and Superclusters

Observations of the cosmic microwave background radiation show matter in the early Universe to be very uniformly distributed, with large-scale density perturbations as small as 1 part in  $10^5$  (Smoot et al. 1992). This is in strong contrast with the present-day Universe and its highly overdense condensations, such as galaxies and clusters of galaxies. A natural and widely accepted explanation for the growth of the density perturbations is that initially slightly overdense regions attract the surround-

ing matter more strongly than underdense regions. Therefore, the expansion of overdense regions is slowed down with respect to underdense regions, and the density contrast grows. Eventually, regions of large enough overdensity can stop their expansion altogether and start recontracting. Their collapse is then followed by a process of relaxation or “virialisation”, after which the resulting object is in an approximate equilibrium state, in which its structure is only occasionally perturbed by merging with other objects. This state is well described by the *virial theorem* of classical mechanics, which states that in such an equilibrium state the gravitational potential energy of the object is proportional to the total kinetic energy of the smaller objects randomly moving inside it (stars in a galaxy, galaxies in a cluster of galaxies). This theorem allows to infer the mass of the object (which determines the gravitational potential) from the measured velocity dispersion and size of the collapsed structure.

Inflationary models for the early Universe predict a well-defined relation between the amplitude of the “initial” density fluctuations on different spatial scales. The prediction, corroborated by several sets of observations, implies that the fluctuations are largest on the smallest scales. Since fluctuations on

all significant scales grow at the same rate, those on the smallest scales will first reach turnaround and virialisation. Thus, the chronological order of formation of objects proceeds from small to large, i.e., from globular clusters<sup>1</sup> to galaxies, groups of galaxies, and finally to galaxy clusters, the largest virialised known structures at present. The next larger objects, namely groupings of clusters of galaxies, or *superclusters*, should presently be undergoing gravitational collapse, whereas even larger structures should still be expanding and only slightly denser than average.

On the largest scales, the Universe is still undergoing a nearly uniform expansion. For a very distant galaxy, its *redshift factor*  $1 + z$ , defined as the ratio of the observed wavelength of a given line in the spectrum to the wavelength of the same line *at its emission*, is a good approximation to the factor by which the Universe expanded in all spatial directions while the radiation was travelling through it. From a Newtonian point of view, applicable to regions much smaller than the Hubble length<sup>2</sup>, this is

<sup>1</sup>Structures much smaller than globular clusters cannot collapse spontaneously, since their gravitational attraction is not strong enough to overcome the pressure of the intergalactic gas. Therefore, stars are formed only within collapsing or already collapsed larger structures.

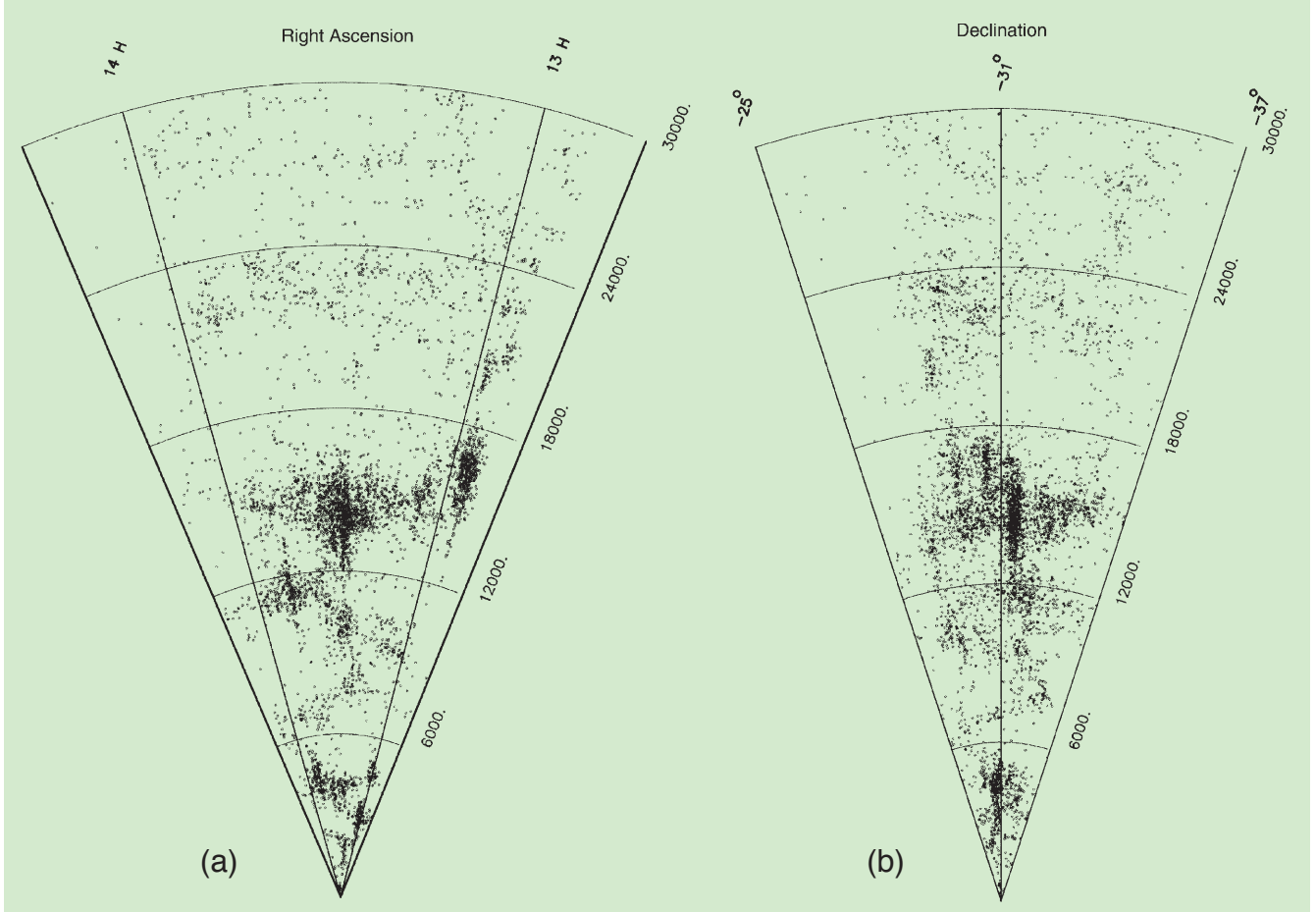


Figure 1: Two projections of the distribution of galaxies with measured redshifts in the region of the Shapley Supercluster. The radial co-ordinate, the recession velocity determined from the redshift,  $cz$ , measured in km/s, is an imperfect surrogate (see text) for the galaxy's distance to us, which would be at the vertex. The angle in panel (a) is right ascension  $\alpha$  in hours ( $1 h = 15^\circ$ ), in panel (b) it is declination  $\delta$  in degrees. Both angles are expanded relative to their true size.

equivalent to write the present-day recession velocity of the galaxy as  $v_r = cz = H_0 d$ , where  $c$  is the speed of light,  $z$  is the same as in the previous definition,  $H_0$  is the Hubble parameter (see footnote 2), and  $d$  is the (Euclidean) distance between us and the object, therefore allowing us to (approximately) infer the distance from the measurement of  $z$ . Knowledge of an object's sky co-ordinates  $\alpha$  and  $\delta$  and its redshift  $z$  allow its approximate positioning in the three-dimensional space, and large catalogues of objects with this information can be used to trace the three-dimensional large-scale structure.

In virialised structures, on the other hand, there is no expansion, and redshift *differences* between constituent objects are due to the local kinematic Doppler effect resulting from relative motions within the structure, which are

unrelated to their distance from us. In this limit, structure along the line of sight is difficult to discern, but the dispersion of redshifts allows to determine the object's mass, as discussed above.

In the intermediate regime, of interest here, the situation is much more murky. Deviations from the uniform expansion are large, some parts of a structure may be expanding while others are contracting at the same time, but no virial equilibrium has been reached. More detailed modelling is generally required to disentangle the three-dimensional morphology and the internal dynamics of the structure. If this can be done, one of its by-products are the masses of these structures, which can be used to constrain the spectrum of initial fluctuations, an important ingredient of all models of cosmological structure formation.

## 2. The Shapley Supercluster

According to recent catalogues of agglomerations of clusters of galaxies (Zucca et al. 1993; Einasto et al. 1997), the so-called Shapley Supercluster is by far the largest such structure in the local Universe, out to  $z \sim 0.1$ . Its core region was first pointed out by Shapley (1930), who noticed a “cloud of galaxies in Centaurus that appears to be one of the most populous yet discovered, [...], oval in form with dimensions roughly  $2.8^\circ$  by  $0.8^\circ$ ”, and centred at the position of the very rich cluster Shapley 8 (Shapley 1933). It was later rediscovered, identified with an X-ray source, called SC 1326-311 (Lugger et al. 1978), and is now more commonly known as A3558 (Abell et al. 1989).

This structure gained attention when a dipole anisotropy in the cosmic microwave background radiation (CMBR) was detected and interpreted as due to the Earth's motion with respect to the homogeneous background frame defined by the CMBR (Smoot & Lubin 1979 and references therein). Correcting for small-scale, local motions, the velocity of the Local Group of galaxies<sup>3</sup> with respect to the CMBR is  $\approx 600$  km/s (e.g., Peebles 1993), approximately in the direction of the structure found by Shapley, but long forgotten.

Initially, it was thought that this motion was produced by the gravitational attraction of the Hydra-Centaurus Super-

<sup>2</sup>The Hubble length is  $c/H_0 \approx 5000$  Mpc, where  $H_0$  is the “Hubble parameter”, i.e., the present expansion rate of the Universe, and 1 Mpc (megaparsec =  $3.086 \times 10^{19}$  km = 3.261 million light-years, roughly the distance between our Galaxy and Andromeda or the size of a cluster of galaxies. The Hubble length is roughly the distance traversed by a light ray during the age of the Universe, much larger than the size of any of the structures being discussed here.

<sup>3</sup>This group contains our own Galaxy (the “Milky Way”), M 31 (“Andromeda”), and 20 or so smaller galaxies, such as M32, M33, and the Magellanic Clouds.

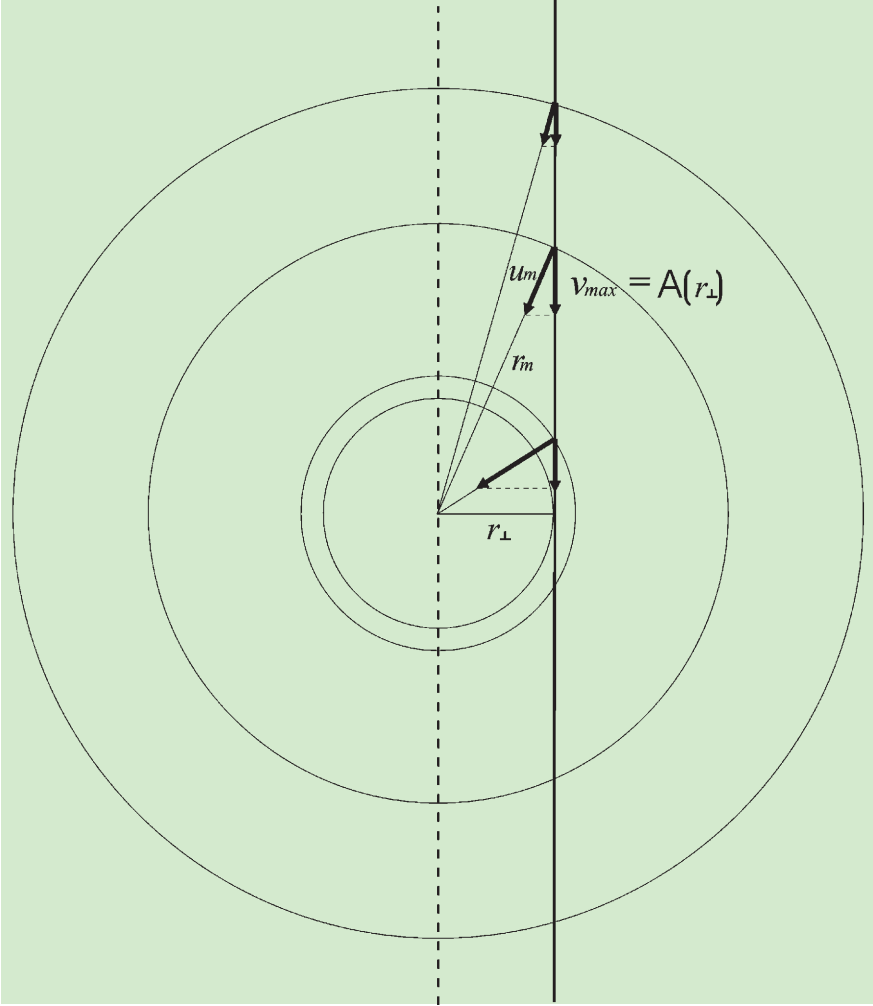


Figure 2: Schematic representation of the spherical collapse model. A discussion is given in the text.

cluster, at  $cz \approx 3000$  km/s. However, Dressler et al. (1987) found a coherent streaming velocity beyond this structure, out to  $cz \approx 6000$  km/s, implying that, if there was one single or dominant “attractor”, this had to be further away. Melnick and Moles (1987), using redshift data gathered in “SC 1326-311” by Melnick and Quintana (1981) and preliminary data taken over a more extended region by Quintana and Melnick (later published in Quintana et al. 1995), showed that there is a much larger concentration at  $cz \approx 14,000$  km/s, which they called the “Centaurus Supercluster”, giving a first mass estimate for its central region, based on the virial theorem, as  $2.5 \times 10^{15} h^{-1} M_\odot$  within  $1^\circ$  or  $\sim 2.5 h^{-1} \text{Mpc}$ ,<sup>4</sup> and finding that this is far from the mass needed, by itself, to produce the required acceleration of the Local Group over the age of the Universe. Scaramella et al. (1989) pointed out that there is a large concentration of clusters in the direction of the Local Group motion, which they called “ $\alpha$ -region”, without reference to either Shapley or Melnick & Moles. It

was Raychaudhury (1989) who pointed out that the concentrations found by all these authors were the same, and coined the name “Shapley Supercluster”. He confirmed a strong concentration of galaxies in that direction, based on a much larger catalogue than that used by Shapley, estimated its total luminosity,  $L$ , and found that an enormous mass-to-light ratio,<sup>5</sup>  $M/L \geq 6000 h M_\odot/L_\odot$ , is required to produce the observed Local Group motion.

We will not attempt to review all the subsequent work carried out on the Shapley Supercluster, but only highlight a few contributions which are important to the present purpose. Spectroscopic observations, with the main purpose of obtaining redshifts, in order to determine masses and trace the 3-dimensional structure of the SSC, were carried out by several groups, but most intensively and systematically by two of them: Quintana and collaborators (Quintana et al. 1995, 1997, 2000; Drinkwater et al. 1999) and Bardelli and collaborators (Bardelli et al. 1994, 1998, 2000, 2001; early work reported in *The Messenger*: Bardelli et al. 1993). Since the SSC is

<sup>4</sup>Here,  $h = H_0/(100 \text{ km/s/Mpc}) \approx 0.5 - 0.8$  is the standard parametrisation of our ignorance regarding the exact value of the Hubble parameter, and  $M_\odot$  is the mass of the Sun,  $2 \times 10^{30} \text{ kg}$ .

<sup>5</sup> $L_\odot = 4 \times 10^{26}$  watts is the luminosity of the Sun. The typical mass-to-light ratio of a cluster of galaxies is  $\sim 300 h M_\odot/L_\odot$  (Peebles 1993).

at declination  $\delta \approx -30^\circ$ , telescopes in Chile are ideally suited for its study. In fact, Bardelli and collaborators have made extensive use of the ESO 3.6-m for a detailed study of the very dense condensations around the clusters A 3558 and A 3528, whereas Quintana and collaborators mostly took advantage of the large field ( $1.5^\circ \times 1.5^\circ$ ) of the 2.5-m telescope at nearby Las Campanas, in order to cover a much wider area,  $\sim 8^\circ \times 10^\circ$ . Their papers discuss quantitative and qualitative properties of individual clusters and the morphology of the SSC (under the assumption that redshifts indicate distances, at least on the global scale of the supercluster). The most detailed discussion so far of the latter was given by Quintana et al. (2000), who find the SSC to consist of several subcondensations with filamentary structures emerging and connecting them. Two projections of the “three-dimensional galaxy distribution” in right ascension  $\alpha$ , declination  $\delta$ , and recession velocity  $cz$  are given in Figure 1.

Different methods have been used to put bounds on the mass and density of parts of the SSC<sup>6</sup>:

(1) adding up the masses of individual clusters determined through the virial theorem (e.g., Quintana et al. 1995, 1997) or from X-ray observations (Raychaudhury et al. 1991; Ettori et al. 1997), which of course gives a lower bound on the total mass, as intercluster matter is not taken into account;

(2) estimates of the overdensity on the basis of galaxy counts on the sky, e.g., in 2 dimensions, having to make educated guesses as to the SSC’s depth and the fraction of the observed galaxies belonging to the SSC as opposed to the foreground or background (Raychaudhury 1989);

(3) estimates of the overdensity from counts in 3-dimensional redshift space, assuming that the redshift is a good distance indicator (Bardelli et al. 1994, 2000), i.e., that the SSC is still in the initial expansion phase; and

(4) virial estimates applied to the whole or a large part of the SSC (Melnick & Moles 1987; Quintana et al. 1995; Ettori et al. 1997), which requires, at least conceptually, that the SSC has already ended its collapse phase and relaxed to an equilibrium state.

We emphasise that methods 3 and 4 place the supercluster at opposite ends of its dynamical evolution, which are both not correct according to the discussion in Section 2. For the sake of argument, consider a homogeneous structure exactly at turnaround. At that instant, there are no internal motions, and all galaxies within the structure are therefore at the same redshift. Analysing this structure with method 3,

<sup>6</sup>We will not go here into the still unresolved and perhaps somewhat academic question of what would be meant by “the whole SSC”. See Quintana et al. (2000) for a recent discussion.

one would argue that there is a finite number of objects within a vanishing volume, and therefore an infinite density would be inferred. With method 4, the vanishing kinetic energy of the structure is taken to reveal a vanishing potential energy, and therefore a vanishing mass density. In practice, this state of zero motion is of course never realised, mostly because superclusters are never homogeneous, but always contain substructure (most prominently clusters of galaxies) whose internal velocity dispersions produce a spread in redshift space, in this way making both estimates give finite results. However, it is not fully clear whether these finite results are close to the true values to be determined<sup>7</sup>. So far, details in the definition of the volume to be considered appear to be more important than the choice of method. The average density within a large radius,  $\sim 10h^{-1}$  Mpc, around the SSC's centre generally comes out to be a few times the cosmological critical density  $\rho_c = 3H_0^2/(8\pi G)$ , not far from the density expected at turnaround ( $\sim 5\rho_c$ ). This makes the discussion above particularly relevant, as more and more data on this and other superclusters are being accumulated.

### 3. Spherical Collapse Models

In order to avoid considering only the extreme limiting cases of pure Hubble expansion or a time-independent equilibrium state, Reisenegger et al. (2000) considered a simplified, spherical model that allows to calculate the full, nonlinear dynamical evolution from the initial (Big Bang) expansion through turnaround until the final collapse. This model, pioneered by Regos & Geller (1989) and applied by them to the infalling galaxies in the outskirts of individual clusters, treats the matter as composed of concentric spherical shells, each of which first expands and then contracts under the gravitational pull of the enclosed matter (composed of the smaller shells). If the structure has an outwardly decreasing density profile, the innermost shells will collapse most rapidly, and no crossing of shells will occur at least until the first shells have collapsed, so the mass  $M$  enclosed in each shell is a constant in time.<sup>8</sup> This allows the time evolution of

<sup>7</sup>Simulations by Small et al. (1998) of superclusters near turnaround within popular cosmological models show at least the virial mass estimate to be surprisingly accurate. It remains to be determined how sensitive this result is to the dynamical state (or density) of the supercluster and to the amount of structure on smaller scales, and whether the galaxy overdensity method is similarly accurate.

<sup>8</sup>Since the density in a (proto-)cluster or supercluster is always much larger than the presently popular value of the "cosmological constant" or "exotic energy" density, the effect of the latter on the dynamics can be safely ignored, except in its contribution to the age of the Universe, i.e., the time available for the collapse to occur.

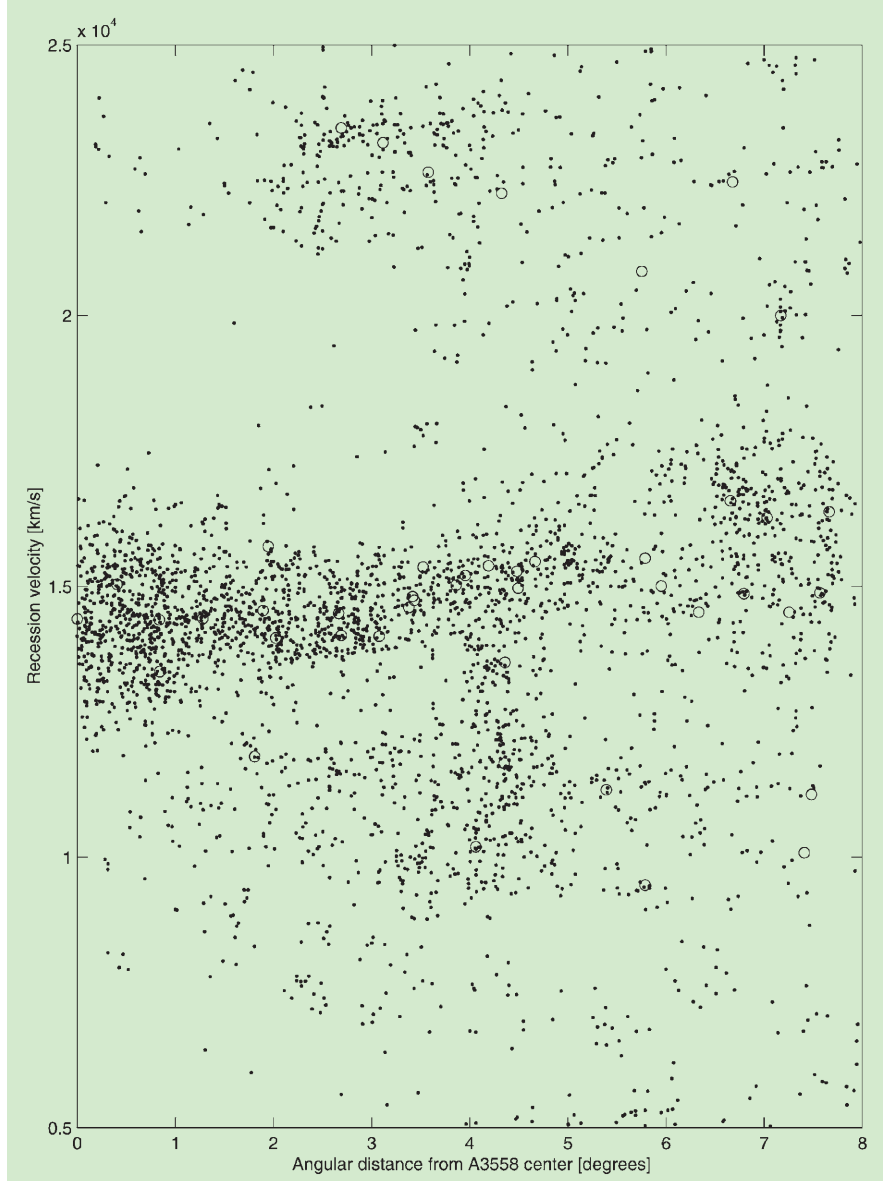


Figure 3: Distribution of galaxies and clusters of galaxies in the Shapley Supercluster, with reference to the central cluster A 3558. The abscissa represents the projected angular distance  $\theta$  of each object to the centre of A 3558, related to the projected physical distance by  $r_1 = 2.5 \theta [degrees] h^{-1}$  Mpc, where our distance to A 3558 is taken to be  $cz/H_0 = 143 h^{-1}$  Mpc. The vertical axis is the line-of-sight velocity,  $cz$ . Dots are individual galaxies, circles represent the centres of clusters and groups of galaxies. Note the dense region extending horizontally from the location of A 3558 (circle at  $\theta = 0$ ,  $cz \approx 14,300 \text{ km s}^{-1}$ ), which is interpreted as the collapsing structure. (Figure reproduced from Reisenegger et al. 2000.)

any given shell's radius,  $r(t)$ , to be written in the familiar parametric form,

$$r = A(1 - \cos \eta); \quad t = B(\eta - \sin \eta); \quad (1)$$

$$A^3 = GM B^2 \quad (1)$$

(e.g., Peebles 1993, chapter 20), where  $A$  and  $B$  are constants for any given shell, determined by the enclosed mass  $M$  and the shell's total energy per unit mass,  $G$  is Newton's gravitational constant, and  $\eta$  labels the "phase" of the shell's evolution (initial "explosion" at  $\eta = 0$ , maximum radius or "turnaround" at  $\eta = \pi$ , collapse at  $\eta = 2\pi$ ). As we are observing many shells at one given cosmic time  $t_1$  (measured from the Big Bang, at which all shells started ex-

panding, to the moment at which the structure emitted the light currently being observed), the speed of each shell can be written as

$$\dot{r} \equiv \frac{dr}{dt} = \frac{r \sin \eta (\eta - \sin \eta)}{t_1 (1 - \cos \eta)^2}. \quad (2)$$

Equations (1) can also be combined to yield

$$M = \frac{r^3 (\eta - \sin \eta)^2}{G t_1^2 (1 - \cos \eta)^3}, \quad (3)$$

the mass enclosed within the shell of current radius  $r$ . Therefore, having an estimate for  $t_1$  (depending on the cosmological model), a measurement of the radial velocity  $\dot{r}$  for each shell would

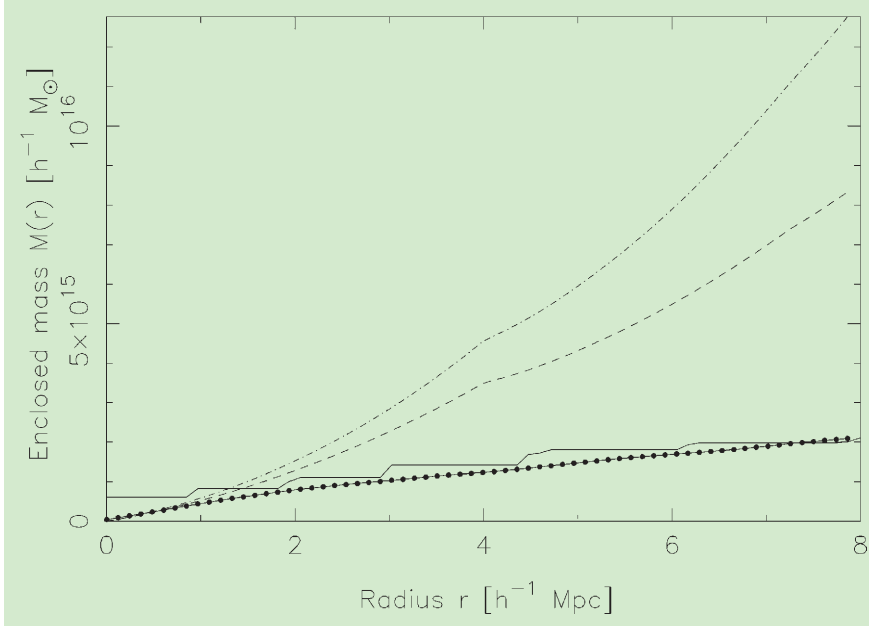


Figure 4: Enclosed mass as a function of radius around A 3558 given by different methods. The solid line is the sum of masses of clusters and groups within the given radius, taking their projected distance as the true distance to A 3558. The dashed and dot-dashed lines are upper bounds to the total mass based on the pure spherical infall model, for a Universe dominated by a cosmological constant and for a Universe with critical matter density, respectively. The solid-dotted line is the estimate from Diaferio & Geller's (1997) escape-velocity model. (Figure reproduced from Reisenegger et al. 2000.)

allow to solve for  $\eta$  and, thus,  $M$  for the same shell. Since redshift measurements yield velocity components along the line of sight, the determination of  $r$  is possible in an indirect and somewhat limited way, as follows.

Along a given line of sight through the collapsing structure, passing at a distance  $r_{\perp}$  from its centre, there can be galaxies at different distances from the observer, whom we take to be at the bottom of Figure 2. A galaxy at the same distance as the centre of the structure falls towards the latter perpendicularly to the line of sight, and therefore has the same redshift as the centre. Galaxies *farther* away from the observer have a velocity component towards the observer, so their redshift is somewhat *lower* than that of the structure's centre. The opposite happens with galaxies closer to the observer (not shown), qualitatively inverting the redshift-distance relation familiar from Hubble's law. The redshift difference between a galaxy and the structure's centre is small both when the galaxy is close to the centre (because the velocity is perpendicular to the line of sight), and when it is far away (because the gravitational pull is weak), so it has to take its extreme (positive or negative) value at an intermediate distance from the centre ( $r_m$  in Fig. 2), thus defining two symmetric "caustics" in redshift space, of amplitude  $v_{max} = A(r_{\perp})$ .

Note that, generally, there will be galaxies also outside the caustics, corresponding to the expanding Universe far away from the collapsing structure. However, the density at the caustics is

formally divergent, and it should also be very high in the enclosed region, making the identification of the caustics relatively unambiguous. Figure 3 shows  $r_{\perp}$  and  $cz$  for the galaxies in the SSC's (projected) central area. The dense region enclosed by the caustics clearly stands out.

The caustics amplitude,  $A(r_{\perp})$ , is a decreasing function of  $r_{\perp}$ , related to the radial velocity,  $\dot{r}(r)$ , by a transformation akin to the Legendre transform familiar from thermodynamics and classical mechanics (Reisenegger et al. 2000, Appendix). This transformation can in general not be directly inverted. Given  $A(r_{\perp})$ , one can in the general case only obtain an upper bound on  $|\dot{r}(r)|$ , and therefore an upper bound on the enclosed mass  $M(r)$ .

Furthermore, as Diaferio & Geller (1997) pointed out, even if the large-scale shape of the structure is roughly spherical, it is expected to have substructure with random velocities. These add to the purely radial infall velocities, washing out the caustics and expanding the redshift range covered by galaxies in the collapsing structure, which further increases the estimated mass. To cure this problem, they propose the alternative relation:

$$M(r) = \frac{1}{2G} \int_0^r A^2(r_{\perp}) dr_{\perp}. \quad (4)$$

There is no rigorous derivation for this result, although it can be justified heuristically by assuming that  $A(r_{\perp})$  reflects the escape velocity at different

radii, i.e., that all galaxies within the dense region are gravitationally bound to the structure. One has to assume further that the radial density profile lies between  $\rho \propto r^3$  and  $\rho \propto r^2$ , as in the outskirts of simulated clusters of galaxies (e.g., Navarro, Frenk, & White 1997). Nevertheless, tests of this model in numerical simulations shows it to work quite well in the infall regions around clusters (Diaferio & Geller 1997; Diaferio 1999).

Figure 4 shows the enclosed mass as a function of radius,  $M(r)$ , as determined by the two methods discussed, together with a third determination, namely the cumulative mass of the clusters enclosed in the given projected radius. The cluster mass estimates,  $M_{500}$ , taken from Ettori et al. (1997) for the most important clusters, are masses within a radius enclosing an average density 500 times the critical density  $\rho_c$ . This is substantially higher than the standard "virialisation density" of  $\sim 200 \rho_c$ , and therefore gives a conservative lower limit to the total virialised mass, which may be increased by a factor  $\sim (500/200)^{1/2} \approx 1.58$  for a more realistic estimate.

Given the simplifications and uncertainties involved, there seems to be fair agreement among the different mass determinations, and it seems safe to say that the mass enclosed by radius  $r = 8h^{-1}$  Mpc lies between  $2 \times 10^{15}h^{-1} M_{\odot}$  and  $1.3 \times 10^{16}h^{-1} M_{\odot}$ , corresponding to a density range  $\rho/\rho_c \sim 3-20$ . It is interesting, nevertheless, that Diaferio & Geller's method gives results that differ so little from the lower limit to the virialised mass in clusters. Therefore, if this method is applicable to the SSC, either there is very little mass outside the clusters of galaxies, or the cluster mass estimates are systematically high.

For comparison, the mass required at the distance of the SSC to produce the observed motion of the Local Group with respect to the cosmic microwave background is  $M_{dipole} \approx 2.8 \times 10^{17}h^{-1} M_{\odot}$ , where a standard value for the cosmological density parameter,  $\Omega_m \sim 0.3$ , has been assumed.<sup>9</sup> The mass within  $8h^{-1}$  Mpc can therefore produce at most  $\sim 5\%$  of the observed Local Group motion, which makes it unlikely that even the whole SSC would dominate its gravitational acceleration. On the other hand, consistent models of the density and velocity distribution on large scales (where density fluctuations are small) in the local Universe can now be built (e.g., Branchini et al. 1999). In these, the SSC figures prominently, although the Local Group motion originates from a combination of several "attractors".

<sup>9</sup> $\Omega_m$  is the ratio of the average mass density in the Universe to the critical density. The required  $M_{dipole}$  is proportional to  $\Omega_m^{0.4}$ .

## 4. Conclusions and Further Work

The SSC is undoubtedly a remarkable structure in a very interesting dynamical state, which deserves further study. A first attempt at a truly dynamical model of the supercluster has been made, but much further progress is possible, at least in principle. A large amount of information is available, namely the sky co-ordinates and redshifts of  $\sim 6000$  galaxies (e.g., Bardelli et al. 2000; Quintana et al. 2000), an important fraction of which is still unpublished, and which is still being expanded, in order to fill in gaps and cover an even wider area (Quintana, Proust et al., in preparation), in order to assess whether a “boundary” of the supercluster can somewhere be discerned. Only a very limited part of the available information, namely the position of the caustics on the  $(r_{\perp}, z)$  plane, has been used in the present spherical collapse models. In principle, the galaxy density at each point on this plane can be used to refine the model, either constraining it more strongly by assuming that the galaxies trace the mass, or determining both the mass density and the galaxy density from the full two-dimensional information (Reisenegger et al., in preparation). However, this will require a uniform redshift catalogue, not available at present, since the available data are a collection of observations taken by different astronomers for different purposes. In order to assess the incompleteness of the present redshift catalogue, a complete and accurate photometric catalogue of the region is being prepared (Slezak et al., in

preparation). A more homogeneous catalogue might also allow to attempt a three-dimensional, non-spherical model of the SSC, perhaps along the lines of recent work on recovering the initial density fluctuations from the present-day redshift-space density distribution in a mildly nonlinear density field (Goldberg & Spergel 2000; Goldberg 2001). Numerical simulations of superclusters can also be run in order to test and calibrate dynamical models to be applied to the SSC.

Our recent research on this topic and the writing of this article were financially supported by the co-operative programme ECOS/CONICYT C00U04, by a 1998 Presidential Chair in Science, and by DIPUC project 2001/06PF.

## References

Abell, G.O., Corwin, H.G. & Olowin, R.P. 1989, *ApJS*, **70**, 1.

Bardelli, S., Scaramella, R., Vettolani, G., Zamorani, G., Zucca, E., Collins, C.A., & MacGillivray, H.T. 1993, *The Messenger*, **71**, 34.

Bardelli, S., Zucca, E., Vettolani, G., Zamorani, G., Scaramella, R., Collins, C.A., & MacGillivray, H.T. 1994, *MNRAS*, **267**, 665.

Bardelli, S., Zucca, E., Zamorani, G., Vettolani, G., & Scaramella, R. 1998, *MNRAS*, **296**, 599.

Bardelli, S., Zucca, E., Zamorani, G., Moscardini, L., & Scaramella, R. 2000, *MNRAS*, **312**, 540.

Bardelli, S., Zucca, E., & Baldi, A. 2001, *MNRAS*, **320**, 387.

Branchini, E., et al. 1999, *MNRAS*, **308**, 1.

Diaferio, A. & Geller, M.J. 1997, *ApJ*, **481**, 633.

Diaferio, A. 1999, *MNRAS*, **309**, 610.

Dressler, A., et al. 1987, *ApJ*, **313**, L37.

Drinkwater, M.J., Proust, D., Parker, Q.A., Quintana, H., & Slezak, E. 1999, *PASA*, **16**, 113.

Einasto, M., Tago, E., Jaaniste, J., Einasto, J., & Andernach, H. 1997, *A&AS*, **123**, 119.

Ettori, S., Fabian, A.C., & White, D.A. 1997, *MNRAS*, **289**, 787.

Goldberg, D.M. 2001, *ApJ*, **552**, 413.

Goldberg, D.M., & Spergel, D.N. 2000, *ApJ*, **544**, 21.

Lugger, P.M., et al. 1978, *ApJ*, **221**, 745.

Melnick, J., & Quintana, H. 1981, *A&AS*, **44**, 87.

Melnick, J., & Moles, M. 1987, *RMxAA*, **14**, 72.

Navarro, J.F., Frenk, C.S., & White, S.D.M. 1997, *ApJ*, **490**, 493.

Peebles, P.J.E. 1993, *Principles of Physical Cosmology* (Princeton: Princeton University Press).

Quintana, H., Ramirez, A., Melnick, J., Raychaudhury, S., & Slezak, E. 1995, *AJ*, **110**, 463.

Quintana, H., Melnick, J., Proust, D., & Infante, L. 1997, *A&AS*, **125**, 247.

Quintana, H., Carrasco, E.R., & Reisenegger, A. 2000, *AJ*, **120**, 511.

Raychaudhury, S. 1989, *Nature*, **342**, 251.

Raychaudhury, S., Fabian, A.C., Edge, A.C., Jones, C., & Forman, W. 1991, *MNRAS*, **248**, 101.

Regos, E., & Geller, M.J. 1989, *AJ*, **98**, 755.

Reisenegger, A., Quintana, H., Carrasco, E.R., & Maze, J. 2000, *AJ*, **120**, 523.

Scaramella, R., Baisi-Pillastrini, G., Chincarini, G., & Vettolani, G. 1989, *Nature*, **338**, 562.

Shapley, H. 1930, *Harvard Coll. Obs. Bull.*, **874**, 9.

Shapley, H. 1933, *Proc. Nat. Acad. Sci.*, **19**, 591.

Small, T.A., Ma, C.-P., Sargent, W.W.L., & Hamilton, D. 1998, *ApJ*, **492**, 45.

Smoot, G.F., & Lubin, P.M. 1979, *ApJ*, **234**, L83.

Smoot, G.F., et al. 1992, *ApJ*, **396**, L1.

Zucca, E., Zamorani, G., Scaramella, R., & Vettolani, G. 1993, *ApJ*, **407**, 470.



**Swimming pool of the Residencia**

The swimming pool at the lowest floor of the Residencia was introduced into the project as a part of the humidification system. However, it also serves as an important psychological element that helps to overcome the harsh living conditions, especially for the permanent staff.  
Photo: Massimo Tarenghi.